World Journal of Gastroenterology

Submit a Manuscript: https://www.f6publishing.com

World J Gastroenterol 2023 July 28; 29(28): 4384-4396

DOI: 10.3748/wjg.v29.i28.4384

ISSN 1007-9327 (print) ISSN 2219-2840 (online)

REVIEW

Advances in application of novel magnetic resonance imaging technologies in liver disease diagnosis

Yi-Ming Qi, En-Hua Xiao

Specialty type: Gastroenterology and hepatology

Provenance and peer review: Unsolicited article; Externally peer reviewed.

Peer-review model: Single blind

Peer-review report's scientific quality classification

Grade A (Excellent): 0
Grade B (Very good): B
Grade C (Good): C
Grade D (Fair): 0
Grade E (Poor): 0

P-Reviewer: Gaspar R, Portugal; Tanaka N, Japan

Received: June 1, 2023
Peer-review started: June 1, 2023
First decision: June 20, 2023
Revised: July 3, 2023
Accepted: July 7, 2023
Article in press: July 7, 2023
Published online: July 28, 2023

Yi-Ming Qi, En-Hua Xiao, Department of Radiology, The Second Xiangya Hospital of Central South University, Changsha 410000, Hunan Province, China

Corresponding author: En-Hua Xiao, PhD, Professor, Teacher, Department of Radiology, The Second Xiangya Hospital of Central South University, No. 139 Renmin Middle Road, Furong District, Changsha 410000, Hunan Province, China. xiaoenhua64@csu.edu.cn

Abstract

Liver disease is a major health concern globally, with high morbidity and mortality rates. Precise diagnosis and assessment are vital for guiding treatment approaches, predicting outcomes, and improving patient prognosis. Magnetic resonance imaging (MRI) is a non-invasive diagnostic technique that has been widely used for detecting liver disease. Recent advancements in MRI technology, such as diffusion weighted imaging, intravoxel incoherent motion, magnetic resonance elastography, chemical exchange saturation transfer, magnetic resonance spectroscopy, hyperpolarized MR, contrast-enhanced MRI, and radiomics, have significantly improved the accuracy and effectiveness of liver disease diagnosis. This review aims to discuss the progress in new MRI technologies for liver diagnosis. By summarizing current research findings, we aim to provide a comprehensive reference for researchers and clinicians to optimize the use of MRI in liver disease diagnosis and improve patient prognosis.

Key Words: Diagnostic imaging; Liver diseases; Fatty liver; Liver fibrosis; Hepatocellular carcinoma; Magnetic resonance imaging

Core Tip: Accurate evaluation of liver disease is essential for effective treatment strategies and better patient prognosis. Magnetic resonance imaging (MRI), a non-invasive diagnostic tool, has become a necessary technique for detecting liver diseases. The advancements in various magnetic resonance techniques have significantly enriched the diagnostic methods for liver diseases, each with a different focus and expertise in examining the liver. This article reviews the principles, advantages, limitations, and clinical applications of these new technologies in the diagnosis of liver disease, providing necessary references for researchers and clinical physicians to enhance the application of MRI in liver disease diagnosis and improve patient prognosis.

Citation: Qi YM, Xiao EH. Advances in application of novel magnetic resonance imaging technologies in liver disease diagnosis. *World J Gastroenterol* 2023; 29(28): 4384-4396
URL: https://www.wjgnet.com/1007-9327/full/v29/i28/4384.htm
DOI: https://dx.doi.org/10.3748/wjg.v29.i28.4384

INTRODUCTION

Liver disease is a major global health concern with high rates of morbidity and mortality[1]. Chronic liver diseases often lead to liver fibrosis and cirrhosis, which are the primary risk factors for hepatocellular carcinoma (HCC)[2]. The accumulation of large molecules such as collagen protein and glycosaminoglycans in the extracellular matrix is the basic pathological feature of liver fibrosis[3]. Reports suggest that 80%-90% of new HCC cases occur in individuals with cirrhosis[4]. Liver cancer is the sixth most common malignancy in humans and the fourth leading cause of cancer-related deaths worldwide. HCC accounts for 90% of all liver cancer cases[5]. Surgery is the preferred method for treating early-stage HCC[6]. However, due to the absence of apparent symptoms in the early stages, most patients are diagnosed late or with distant metastasis[7]. In major Western centers, the incidence of HCC recurrence within 5 years after curative liver resection is estimated to be 60%-70%[8]. Therefore, early diagnosis and recurrence monitoring are crucial for these patients.

Imaging examinations are vital in diagnosing chronic liver disease and liver cancer. HCC can be diagnosed non-invasively without requiring pathological confirmation, unlike most solid tumors[9]. MRI is a commonly used imaging technique that provides detailed information on the pathological and physiological aspects of liver cancer. It reflects changes in the tissue structure, metabolic status, tumor microenvironment, and other relevant factors.

Recent advancements in magnetic resonance imaging (MRI) technology, such as diffusion weighted imaging (DWI), intravoxel incoherent motion (IVIM), magnetic resonance elastography (MRE), chemical exchange saturation transfer (CEST), magnetic resonance spectroscopy (MRS), hyperpolarized MR (HP MR), contrast-enhanced MRI (CE-MRI), and radiomics, have significantly improved the accuracy and effectiveness of liver disease diagnosis. These new technologies are expected to provide further important information on tumor biological behavior.

This review aims to discuss the progress in new MRI technologies for liver disease diagnosis. By summarizing current research findings, we aim to provide a comprehensive reference for researchers and clinicians to optimize the use of MRI in liver disease diagnosis and improve patient prognosis.

NEW MRI TECHNOLOGIES FOR LIVER DISEASE DIAGNOSIS

DWI and IVIM

DWI is a non-invasive imaging technique that provides information on liver tumors, diffuse liver lesions, and liver function status without the need for contrast agents[10]. DWI has become a popular tool in tumor chemotherapy response assessment and follow-up after treatment due to its ability to detect recurrent lesions earlier than traditional imaging techniques[11].

IVIM, an extension of DWI, has shown great potential in liver function assessment[12], diagnosis of diffuse liver lesions [13] and liver tumors, and liver lesion characterization[14]. It is commonly used to estimate blood flow and microvascular perfusion[15]. The IVIM analysis includes the D value (representing pure diffusion factors), the $D*$ value (representing transport and perfusion factors), and the f value (representing microvascular perfusion factors). Research has demonstrated that IVIM has a higher diagnostic efficacy for displaying different liver lesions than DWI. Additionally, the diagnostic efficacy of the D value derived from IVIM is significantly higher than that of the apparent diffusion coefficient (ADC) value[16]. IVIM can also be used to predict histological grade, as the D value exhibits good diagnostic performance in distinguishing high-grade from low-grade liver cancer[17].

The perfusion-diffusion ratio (PDR) is a recent concept proposed to enhance the effectiveness of DWI. PDR is the ratio of the decreased signal rate caused by IVIM to the decreased signal rate caused by diffusion. A study was conducted to compare the effectiveness of IVIM parameters, ADC value, and PDR in distinguishing solid benign and malignant liver diseases in patient imaging data. The results indicate that PDR had better accuracy compared to IVIM parameters and the ADC value, with an accuracy rate of 79%, while also exhibiting high sensitivity and specificity[18].

The technologies of DWI and IVIM show great promise in aiding the diagnosis and treatment of liver cancer. Furthermore, the introduction of PDR has provided new insights for DWI, allowing for a more precise evaluation of liver cancer. However, DWI does have some limitations, such as the low repeatability of the ADC value, which prevents it from being a dependable imaging biomarker[19]. In addition, DWI is prone to several artifacts such as blurring, ghosting, and distortion which pose a challenge in achieving the repeatability of IVIM parameters and the ADC value[20]. To address this issue, Simchick *et al*[21] proposed a two-dimensional (2D) *b*-M1-optimized data acquisition technique that offers better stability and repeatability in measuring IVIM parameters. This technique can be instrumental in establishing IVIM quantitative biomarkers for liver disease.

MRE

Liver biopsy is widely accepted as the most reliable method for diagnosing and staging liver fibrosis[22]. However, its invasiveness, cost, and potential for complications limit its use. Furthermore, the diagnostic reliability of liver biopsy is questionable due to its sampling variability and subjectivity[23]. Ultrasound elastography is a low-cost and easy-to-use alternative, but it is highly influenced by obesity[24]. For example, vibration-controlled transient elastography (VCTE) is one of the most widely used ultrasound-based methods for diagnosing liver fibrosis. Its rapid, safe, and reproducible nature has made it widely used for bedside diagnosis. However, its reliability is lower than that of MRE as 15% of its conclusions are inaccurate, which is mainly due to the impact of obesity and insufficient experience of doctors[25,26]. According to a large sample meta-analysis, the summary area under the curve (AUC) values of VCTE for diagnosing significant fibrosis, advanced fibrosis, and cirrhosis were lower than those of MRE, with values of only 0.83, 0.85, and 0.89, respectively, while MRE had AUC values as high as 0.91, 0.92, and 0.90, respectively[27]. Serum biomarkers have also been explored for liver fibrosis evaluation, but their lack of specificity poses a challenge as they may also be released during inflammation in other tissues[28].

MRE proves to be a better method for diagnosing and staging liver fibrosis as it is not influenced by factors such as obesity, ascites, inflammation, or etiology[29]. The accuracy and reliability of MRE in diagnosing all stages of liver fibrosis, especially late-stage fibrosis and cirrhosis, have been confirmed by multiple meta-analyses[27,30]. However, the clinical application of MRE is still restricted due to its long examination time and high cost.

Encouragingly, recent studies suggest that combining serum biomarkers and MRE could have unexpected benefits. For instance, fibrosis-4 (FIB-4) index, an indicator used to assess liver injury and fibrosis, includes aspartate aminotransferase, alanine aminotransferase, age, and platelet count[31]. Tamaki *et al*[32] conducted a study where they used a two-step strategy combining FIB-4 index and MRE to detect late-stage fibrosis. They found that the accuracy of the two-step strategy was equivalent to that of using MRE alone, which could lead to cost reduction by reducing excess MRE. Therefore, the two-step strategy can serve as a screening method for large populations. Another study also demonstrated that the combined use of MRE and FIB-4 index has excellent negative predictive value in liver decompensation, which has significant clinical implications[33]. In addition, MRE has acceptable specificity and sensitivity in evaluating splenic stiffness and portal hypertension[34], which is crucial for assessing the overall health status of patients with cirrhosis.

Currently, liver fibrosis assessment can be carried out using 2D MRE, but a more advanced option now available is three-dimensional (3D) MRE. Unlike 2D MRE, 3D MRE images allow analysis of the entire volume of the liver in a 3D manner, providing better accuracy by collecting and processing information in all directions. In a study by Li *et al*[35], the diagnostic performance of 2D MRE and 3D MRE was compared, and both were found to have strong performance in detecting and staging liver fibrosis. However, 3D MRE provided significantly better image quality than the 2D MRE method and had higher inter-observer consistency in measuring liver stiffness (LS). Furthermore, in their study, Catania *et al*[36] found that 3D MRE is more repeatable due to its lower sensitivity to artifacts and provides a more comprehensive liver evaluation by including a larger area of liver parenchyma.

MRE has been found to be useful in predicting the occurrence and recurrence of HCC. Reports suggest that the risk of developing HCC increases with LS as measured by MRE[37]. Late-stage HCC recurrence is predicted by LS ($P < 0.001$), which has a high specificity (90.0%)[38]. MRE has also shown potential in diagnosing microvascular invasion (MVI) in HCC. A study by Zhang *et al*[39] found that tumor stiffness (TS) increased with MVI severity, with TS/LS > 1.47 ($P = 0.001$), TS > 4.33 kPa ($P < 0.001$), and irregular tumor margins ($P = 0.006$) being important independent predictors of MVI positivity.

In summary, MRE is a valuable tool for the thorough evaluation of liver fibrosis, cirrhosis, HCC, and portal hypertension in individuals with liver disease. Although MRE has demonstrated high accuracy in identifying advanced fibrosis or cirrhosis, there are discrepancies in the diagnostic threshold for fibrosis staging based on retrospective data meta-analyses[40], which require further validation.

CEST MRI

The CEST technique, first introduced by Ward *et al*[41] in 2000, utilizes off-resonance saturation pulses to saturate a specific substance, which in turn affects the signal intensity of free water through chemical exchange, providing relevant information about the substance. There are several types of CEST, including Glu CEST, Cr CEST, LATEST, and Gluco CEST, which can, respectively, map glutamate, creatine, lactate, and glucose, all of which are important substances involved in tumor metabolism. CEST can be divided into two categories: Exogenous CEST and endogenous CEST, depending on whether exogenous CEST agents are used. In liver imaging, CEST MRI can be used to evaluate tumor metabolism and tumor microenvironment, and monitor tumor treatment response.

Tumors are known to exhibit increased glucose uptake and glycolysis. To monitor tumor glucose metabolism and treatment response, ^{18}F-fluorodeoxyglucose positron emission tomography (^{18}F-FDG PET) is commonly used. However, the high cost and radioactivity of this method limit its application. CEST MRI has emerged as a potential alternative. A study by Chan *et al*[42] showed that using D-glucose, a simple carbohydrate, to detect tumor metabolism was possible.

The Gluco CEST image showed a significant enhancement in the tumor region, consistent with PET results. However, the CEST signal decreases rapidly due to the rapid metabolism of D-glucose after entering the cells[43]. In recent years, 3-O-methyl-D-glucose (3OMG) has emerged as a promising option for monitoring tumor progression and treatment efficacy. Unlike D-glucose, 3OMG is not metabolized after being taken up by cells, and accumulates in tumor cells, giving it a different kinetic profile[44]. Its similar CEST contrast efficiency to D-glucose makes it a suitable reporter for tumor cell glucose transporters. The Gluco CEST technique, which utilizes 3OMG, offers a low-risk option for patients with renal diseases to display tumor metabolism without using radioactive tracers.

In addition, CEST MRI provides a non-invasive method for evaluating tumor pH, which is important due to the Warburg effect. This effect leads to increased lactate production within cancer cells and results in an acidic extracellular pH in the tumor microenvironment. This acidic environment can enhance tumor invasiveness, metastasis, angiogenesis, and resistance to radiotherapy and chemotherapy[45]. The CEST measurement of pH is not limited by observation depth and can be used for whole-body imaging. While amide proton transfer (APT) CEST MRI is capable of measuring pH[46], it is limited in its ability to calculate the absolute value of pH. To address this limitation, exogenous agents have been utilized to measure extracellular pH in the tumor microenvironment. The use of iodinated agents in CEST MRI has emerged as a promising non-invasive technique for pH assessment[47], as these clinically approved agents are not affected by concentration and offer advantages over APT MRI.

CEST has found another novel application in image-guided nanoparticle (NP) drug delivery. This technique can monitor the transformation and distribution of NP drugs in the body, thereby assisting in adjusting treatment plans. CEST-guided NP drug delivery systems can be divided into labeled and unlabeled systems, depending on the labeling strategy used to achieve the CEST signal[48]. For example, Law *et al*[49] successfully used CEST MRI to detect the specific distribution of iohexol-labeled liposome drugs in the brain of an animal model. In a separate study, Liu *et al*[50] introduced a new labeling-free strategy that uses CEST MRI imaging technology to detect the delivery efficiency of anti-cancer drug lentinan-functionalized SeNPs and achieve image-guided drug delivery. The ability of CEST MRI to visualize NP drug delivery provides a unique opportunity for the integration of tumor diagnosis and treatment. However, this technology is still in its infancy, and nearly all related research is currently being conducted in preclinical animal models. Therefore, extensive validation is necessary to ensure its accuracy and acceptability for clinical translation.

CE-MRI

CE-MRI is a technique used to enhance liver lesion imaging by injecting a contrast agent intravenously. The contrast agent distribution patterns in the liver can be classified into four categories[51]: (1) Extracellular fluid agents, such as Gd-DTPA and Gd-DOTA, rapidly enter the hepatic capillary network and diffuse into the tissue space after injection, eventually being excreted by the kidneys; (2) Hepatobiliary agents, such as Gd-EOB-DTPA and Gd-BOTPA, can be absorbed and metabolized by normal liver cells. During the hepatobiliary phase, regions with premalignant liver lesions or malignant tumors display low signal due to decreased contrast agent uptake[52]; (3) Superparamagnetic iron oxide (SPIO) particles can be taken up by Kupffer cells in normal liver tissue, resulting in a 'black liver' effect. Tumor tissue displays high signal because it almost does not take up SPIO particles; and (4) Molecular targeted MRI contrast agents can be modified with specific antibodies or ligands, allowing them to bind specifically to tumor tissue and highlight the tumor.

The development of MRI contrast agents with tumor targeting, safety, and efficacy has been extensively researched. The use of molecular targeted MRI contrast agents with specific antibodies or ligands has shown promising results in actively targeting tumor tissue, enabling early detection of tumors. Various specific targets can be utilized to produce specific contrast agents. This review will introduce glypican-3 (GPC3) and alpha-fetoprotein (AFP) as examples.

GPC3 is a cancer embryonic polysaccharide present on the cell membrane. Studies have shown that GPC3 is highly expressed in over 70% of HCCs, but not in hepatitis, cirrhosis, benign liver lesions, or healthy adult tissue. GPC3 promotes the progression of liver cancer by binding to molecules such as Wnt signaling proteins and growth factors[53]. In terms of diagnosis, GPC3 has a diagnostic specificity similar to AFP but with higher sensitivity[54]. Additionally, GPC3 can be used to distinguish AFP-negative HCC[55], making it a more reliable diagnostic marker for HCC. Overall, GPC3 shows promise as a potential diagnostic tool for HCC. Zhao *et al*[56] have developed a novel liver cancer-targeting probe by combining USPIO with GPC3-specific ligands. The probe demonstrated preferential binding to GPC3 in both *in vitro* and *in vivo* experiments. Furthermore, it exhibited good stability and biocompatibility, making it a promising candidate for a targeted MRI contrast agent.

AFP is not typically expressed in adults, but in liver cancer patients. AFP levels may be very high, making it a potential target for detecting liver cancer[57]. AFP antibodies can be used to create targeted probes, but as previously mentioned, AFP is not highly expressed in all liver cancer patients. To address this issue, Ma *et al*[58] conjugated AFP antibodies and GPC3 antibodies to ultra-small SPIO NPs (USPIO), resulting in the development of a dual-antibody-conjugated MRI probe that can detect heterogeneity and small HCC with higher sensitivity than single-target probes. The experiment demonstrated that using dual-antibody-conjugated USPIO probes for targeting cancer cells was more efficient and sensitive compared to using single-labeled probes that targeted AFP-USPIO and GPC3-USPIO, as well as non-targeted USPIO. This finding highlights the potential of using multi-target probes to overcome tumor heterogeneity and improve sensitivity to HCC.

Gadolinium-based contrast agents (GBCAs) are commonly used in MRI, but they carry the risk of allergic reactions and nephrogenic systemic fibrosis[59]. Furthermore, even patients with normal kidney function can experience gadolinium accumulation in all tissues with GBCA exposure[60]. Therefore, the development of effective Gd-free MRI contrast agents is becoming increasingly important. Manganese (Mn) has emerged as a promising alternative to GBCAs[61], with researchers discovering that Mn oxide nanoparticles have negligible toxicity and produce good T1-weighted contrast effects[62]. Mn^{2+} has also demonstrated potential as an anti-cancer drug or adjuvant, making it a fascinating area of

research[63]. In a recent study, researchers found that administering Mn^{2+} to a mouse model induced a strong systemic anti-cancer response. This was achieved through promoting natural killer cell function, macrophage and dendritic cell maturation and activation, CD8+ T cell differentiation and activation, and memory T cell survival in tumors. As a result, tumor growth and metastasis were greatly inhibited. Another group of researchers developed an intelligent therapeutic probe called MnTBs, which decomposes quickly in acidic and reducing cellular environments, releasing Mn^{2+} and triggering chemodynamic therapy. This probe was found to be effective in inhibiting tumor growth and metastasis, as well as detecting millimeter-sized liver metastases with a high contrast of 316%[64]. These findings suggest that Mn-based contrast agents have potential in targeted tumor therapy.

MRS

MRS is a non-invasive method that monitors organ metabolites, making it particularly suitable for the liver due to its high concentration of multiple metabolites such as ATP, glutamine, and glycogen. The liver MRS analysis primarily uses ^{1}H, ^{31}P, and ^{13}C. Its major applications include the diagnosis and grading of fatty liver and liver fibrosis, as well as the diagnosis of liver tumors.

The incidence of non-alcoholic fatty liver disease (NAFLD) is increasing, and some patients with NAFLD may develop non-alcoholic steatohepatitis, which can progress to liver cirrhosis and HCC[65]. Therefore, early diagnosis is crucial for preventing and treating NAFLD. ^{1}H-MRS is a non-invasive method that can accurately measure the content of triglycerides in the liver[66]. However, it has some limitations, such as long processing time, motion artifacts, and sampling errors.

The use of MRI proton density fat fraction (MRI-PDFF) has become a popular method for measuring liver fat content in recent years[67]. MRI-PDFF has a strong correlation with MRS ($r = 0.983$, $P < 0.001$) and can quantitatively measure the lipid content of the entire liver[68], overcoming the limitations of MRS and liver tissue biopsy. This makes MRI-PDFF a widely used reference standard for image-based fat quantification with broader application prospects than MRS[69]. In addition, the recent use of the multi-echo Dixon sequence has shown promising results in detecting NAFLD[70].

In the diagnosis and staging of liver fibrosis, ^{1}H-MRS and ^{31}P-MRS have distinct values. Ding *et al*[71] discovered that choline (Cho) levels measured by ^{1}H-MRS increased in proportion to the severity of liver fibrosis. They also found that the Cho/lipid ratio was the most significant diagnostic indicator of liver fibrosis based on the receiver operating characteristic curve. The diagnostic thresholds for liver fibrosis and early cirrhosis were ≥ 0.028 and ≥ 0.131, respectively. In comparison to ^{1}H-MRS, ^{31}P-MRS is advantageous in diagnosing cirrhosis as it can distinguish between different causes of liver disease. Through quantitative analysis of metabolite concentrations such as phosphate monoester (PME), phosphate diester (PDE), Pi, and ATP, ^{31}P-MRS has the potential to differentiate between alcoholic liver disease, viral liver disease, NAFLD, and cirrhosis[72]. However, larger-scale multi-center studies are needed to confirm the clinical relevance and usefulness of this finding.

Liver cancer patients can benefit from the use of ^{1}H-MRS and ^{31}P-MRS as well. In ^{1}H-MRS, the Cho peak is a significant indicator of focal liver lesions, and its elevation could suggest the proliferation of tumor tissue due to increased synthesis of cell membrane phospholipids. Furthermore, the information provided by the Cho peak can be further developed. Liao *et al*[73] conducted a study to compare the diagnostic performance of Cho peak area, Cho peak amplitude, and combined methods for early detection of rabbit liver cancer. The results showed that the combined method had higher accuracy in the early diagnosis of liver cancer, and the correlation between Cho peak amplitude and tumor volume was the best. In ^{31}P-MRS, the contents of PME and PDE can reflect cell membrane synthesis and breakdown, and their increase means cell proliferation. Liver tumors can be associated with an increase in PME/PDE and PME/Pi, and changes in PME/PDE after treatment are significant. However, further multi-center studies are needed to confirm their accuracy due to high heterogeneity[74]. ^{31}P-MRS is also reliable for measuring ATP consumption and identifying the degree of acute liver ischemia-reperfusion injury (IRI)[75], which is particularly meaningful for patients who require hepatectomy and liver transplantation. Diagnosis and treatment of IRI during surgery have always been a challenging task.

^{13}C MRS is considered the gold standard for imaging human liver glycogen metabolism after oral ingestion of ^{13}C-labeled glucose[76]. However, the low natural abundance and sensitivity of ^{13}C nuclei can limit their application. To overcome this challenge, researchers have developed hyperpolarization techniques, which will be discussed below. For readers' convenience, the targets of MRS and HP MR in liver metabolism evaluation are summarized in Figure 1.

However, motion still has an impact on the accuracy of MRS. Additionally, liver tissue has significant heterogeneity, so excluding extraneous tissue when setting the observation area is crucial. As technology continues to advance, MRS is expected to become an increasingly important tool for diagnosing and grading liver tumors, potentially replacing the need for invasive biopsies.

HP MR

The development of HP MR can be attributed to the dynamic nuclear polarization (DNP) technique, which was initially proposed by Ardenkjaer-Larsen *et al*[77]. This technique can increase MR signal by more than 10000 times. Currently, the leading HP biomarkers primarily consist of ^{13}C, with [1-^{13}C] pyruvate being the most commonly used due to its central role in cellular metabolism. When absorbed by liver cells, [1-^{13}C] pyruvate can produce three observable metabolic intermediates: Lactate, alanine, and CO_2, thus allowing visualization of liver metabolism.

Cancer cells often have higher levels of the enzyme lactate dehydrogenase[78], which convert pyruvate to lactate. Measuring the metabolic transformation from pyruvate to lactate is important for analyzing tumor invasiveness, grade, and prognosis[79]. In a study, HCC was induced in rats, and tumor cells were extracted and re-implanted into another group of nude mice. The study found that tumors re-implanted from cells with higher lactate/pyruvate ratios showed higher lactate signals. Therefore, using HP MR to evaluate glucose metabolism differences in liver cancer tissue could potentially reveal tumor phenotypes[80].

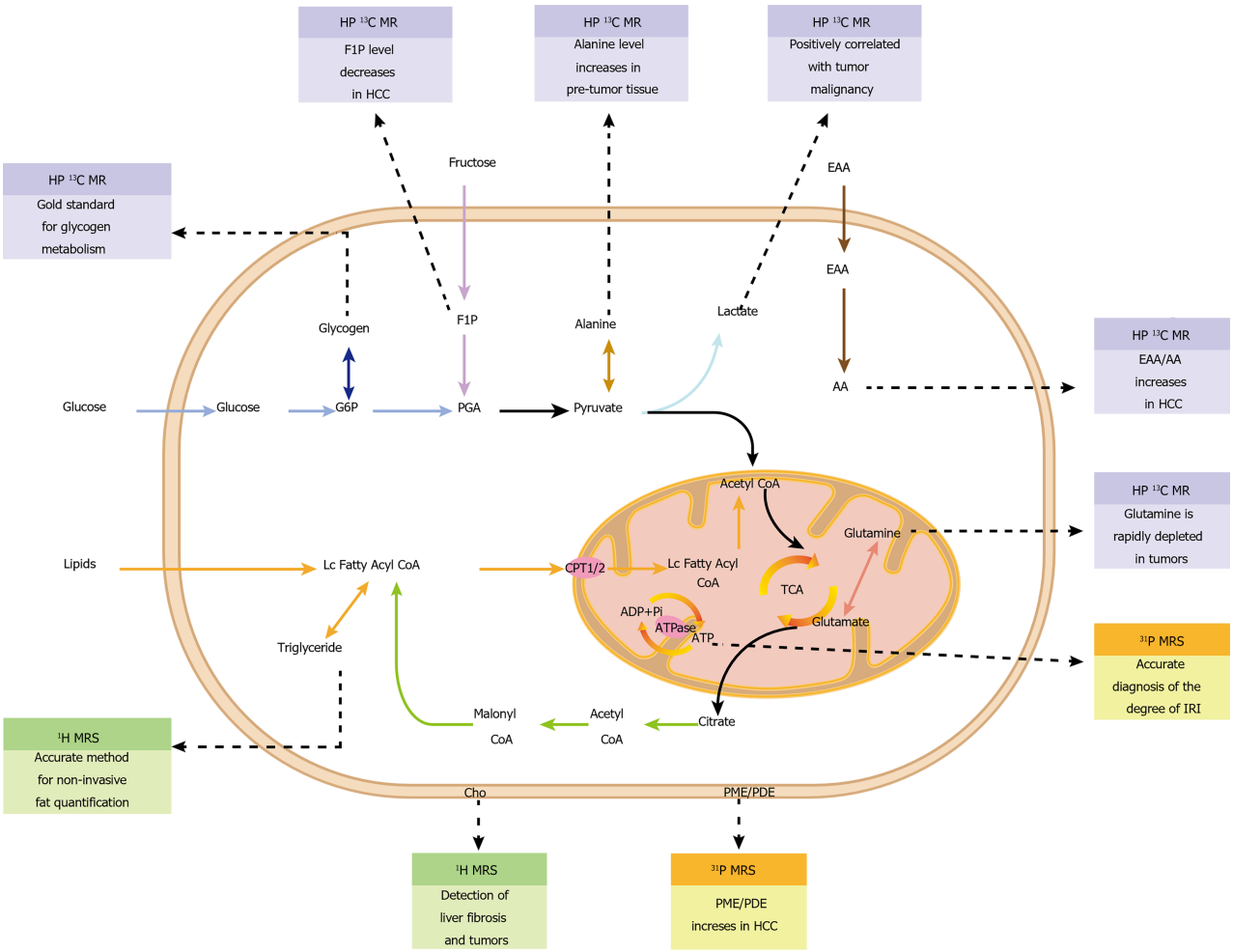

DOI: 10.3748/wjg.v29.i28.4384

Figure 1 The targets of magnetic resonance spectroscopy and hyperpolarized magnetic resonance in liver metabolism evaluation. AA: Acetoacetate; CPT: Carnitine palmitoyl transferase; Cho: Choline; EAA: Ethyl acetoacetate; F1P: Fructose-1-phosphate; G6P: Glucose-6-phosphate; IRI: Ischemia-reperfusion injury; HCC: Hepatocellular carcinoma; PDE: Phosphate diester; PGA: Phosphoglyceric acid; PME: Phosphate monoester; TCA: Tricarboxylic acid; MRS: Magnetic resonance spectroscopy.

Alanine is another potential biomarker for liver cancer diagnosis. It was found that an increase in alanine generation was the earliest metabolic change detected in liver cancer models, even before the formation of primary tumors. In pre-tumor tissues, the conversion rate of pyruvate to alanine significantly increased, and the area with the most abundant alanine signal in pre-tumor tissues was often the region where tumor nodules form[81]. Thus, [1-^{13}C] pyruvate HP MR can be used for early diagnosis of liver cancer by monitoring alanine generation.

Recent studies have shown an increased interest in the use of other hyperpolarization probes, including HP [1,3-$^{13}C_2$]-ethyl acetoacetate, HP [2-^{13}C]-fructose, and HP [5-^{13}C, 4,4-$^{2}H_2$,5-^{15}N]-L-glutamine. Ethyl acetoacetate (EAA) is converted to acetoacetate (AA) at a reduced rate in HCC cells due to lower concentrations and activity of carboxylesterases. In a rat liver transplant tumor model, HP [1,3-$^{13}C_2$]-ethyl acetoacetate MR revealed that the EAA/AA ratio in tumor tissue was approximately four times higher than that in healthy tissue (P = 0.009)[82]. Similarly, HP [2-^{13}C]-fructose can be used to explain HCC cell metabolism. HCC cells have reduced generation of fructose-1-phosphate (F1P) due to lower expression of ketohexokinase[83]. HP MR has successfully detected F1P and its loss in an HCC model. Finally, evaluation of glutamine metabolism is also beneficial for liver cancer diagnosis because it is rapidly consumed by proliferating cells in tumor tissue. The newly developed HP [5-^{13}C, 4,4-$^{2}H_2$,5-^{15}N]-L-glutamine proved to be the best choice for determining *in vivo* glutamine metabolism[84].

Importantly, HP MR provides a unique advantage in obtaining information on tumor metabolism and perfusion, which is not easily obtainable through other methods. The latest technology utilizes the dual-probe imaging method, which involves the use of [1-^{13}C]-pyruvate and [^{13}C, $^{15}N_2$]-urea for simultaneous tumor perfusion and metabolic imaging [85]. The metabolic conversion rate of pyruvate indicates enzyme activity and transporter expression, whereas HP ^{13}C urea is a non-metabolically active extracellular probe that reflects tissue perfusion and distribution. The combination of these two probes can effectively explain changes in metabolism and perfusion during disease progression and treatment response.

PET is currently the preferred imaging method in clinical practice as it provides metabolic information through non-invasive analysis of cancer metabolism *in vivo*. This is achieved through the injection of ^{18}F-FDG[86]. Although PET is

useful for assessing glucose metabolism, it has limited ability to evaluate downstream metabolism, which can be important in many cases. However, HP ^{13}C-pyruvate MR can provide information about downstream metabolism. To obtain a complete picture of glucose metabolism, a combination of ^{18}F-FDG and [1-^{13}C] pyruvate methods can be used. Hansen *et al*[87] have demonstrated the feasibility of this approach through a technique called hyperPET, which shows the consistency between tumor ^{18}F-FDG uptake and [1-^{13}C] lactate production. Clemmensen *et al*[88] have also shown that combining [^{68}Ga]Ga-NODAGA-E[(cRGDyK)]$_2$ PET and HP [1-^{13}C]-pyruvate MR can enhance the ability of hyperPET to detect tumor angiogenesis. HyperPET is a promising tool for evaluating glucose metabolism direction in order to predict tumor occurrence and evaluate the malignancy degree of the tumor. It achieves this by describing the transformation of pyruvate into alanine, lactate, or entering oxidative phosphorylation in the body. While the complexity and high cost of hyperPET may seem impractical for routine use, advancements in MRI and PET-related technologies may make it a valuable tool for diagnosing liver cancer.

Recent advancements in HP MR have led to improvements in both efficiency and accuracy. The slow production of hyperpolarized pyruvate using DNP has been addressed with the MINERVA protocol, which has greatly facilitated the clinical translation of HP MR[89]. Additionally, quantification bias resulting from the use of surface transmit/receive coils has been addressed by Lee *et al*[90] through the development of a dedicated HP ^{13}C EPSI post-processing pipeline. This method has significantly improved the accuracy of measuring the pyruvate to lactate conversion rate in tumors and adjacent regions, with the average signal-to-noise ratio of pyruvate, lactate, and alanine increased by 37.4, 34.0, and 20.1 times, respectively.

MRI radiomics

The concept of radiomics was introduced by Lambin *et al*[91] in 2012. This method involves extracting features from conventional imaging at the tumor's overall level, providing a non-invasive, comprehensive, and quantitative observation of the tumor's temporal and spatial heterogeneity. Presently, MRI-based radiomics research in the liver primarily focuses on classification of liver fibrosis and hepatitis, liver cancer diagnosis, differentiation degree and immunohistochemistry prediction, and MVI evaluation.

MRI-based radiomics has shown promise in diagnosing and predicting hepatitis and liver fibrosis. While conventional MRI images can detect severe cases by observing changes in water content and distribution caused by inflammation, subtle tissue changes can prove challenging to diagnose. Radiomics technology can capture these tiny changes, allowing for more accurate diagnosis. Wei *et al*[92] proposed a grading system that simultaneously stages fibrosis and inflammation activity, with an AUC of 0.932 and 0.910 for diagnosing early-stage hepatitis and fibrosis, respectively. This study demonstrates the potential for radiomics to improve diagnosis and prediction of liver diseases. A novel technique, known as the dynamic image radiomics model, has been developed using deep learning technology to evaluate liver fibrosis. This method combines imaging features from multi-phase dynamic contrast-enhanced images with temporal features. It utilizes time-varying curves of contrast enhancement and imaging features during enhancement and eliminates manual selection bias by using an automated region of interest extraction method. Overall, compared with traditional radiomics methods and clinical serum parameters, the dynamic radiomics model has stronger predictive performance for various stages of liver fibrosis. The proposed liver fibrosis classification model is highly automated, saving time and effort. This model is significant in predicting new cases and training additional datasets[93].

Research has shown that MRI-based radiomics models are highly effective in distinguishing between HCC and non-HCC, with better discrimination efficiency than visual assessment by novice radiologists ($P < 0.05$)[94]. These models also have significant value in identifying high- and low-grade HCC. In a study by Ameli *et al*[95], radiomics features demonstrated strong differentiation ability in a multi-classification model, with an AUC of 0.83. This outperformed classification based solely on ADC or arterial-phase enhancement value, which had an AUC of only 0.75.

Moreover, research has shown that MRI radiomics features have good predictive efficacy for immunohistochemistry and molecular expression in HCC. For example, CK19+ HCC has higher invasiveness, higher lymph node metastasis rates, higher resistance to radiotherapy and chemotherapy, and poorer prognosis. Researchers have successfully constructed and validated a multi-sequence radiomics model for accurately identifying the CK19 status of HCC patients using multi-center MRI imaging data[96]. GPC3 is also associated with poor prognosis in HCC patients. Gu *et al*[97] developed a useful method for predicting GPC3 positive HCC patients without invasive procedures by combining AFP and radiomics features in a column chart. The tool showed significant predictive performance in both training and validation cohorts, with AUC values of 0.926 and 0.914, respectively. Additionally, radiomics features were found to be correlated with the protein level of the immunotherapy target programmed cell death ligand 1 (r = 0.41-0.47, $P < 0.029$) and the mRNA expression levels of programmed cell death 1 and cytotoxic T-lymphocyte-associated protein 4 (r = -0.48 to 0.47, $P < 0.037$)[98]. The findings of these studies indicate that utilizing a combination of multi-sequence MRI radiomics features can lead to precise classification of immunohistochemistry and molecular expression in liver cancer. This non-invasive approach can facilitate personalized management strategies for patients.

The use of MRI radiomics analysis can also provide a distinct advantage in preoperative diagnosis of MVI in liver cancer, as current diagnosis of MVI can only be made through postoperative histological examination. Feng *et al*[99] developed an MRI radiomics model for predicting preoperative MVI by extracting radiomics features from Gd-EOB-DTPA-enhanced MRI. The model's AUC, sensitivity, and specificity were 0.83, 90%, and 75%, respectively, which outperformed radiologists in predicting MVI. According to Liang *et al*[100]'s meta-analysis of 15 studies and 981 patients, MRI radiomics has a high accuracy in diagnosing MVI with an AUC of 0.87, sensitivity of 79%, and specificity of 81%. Based on our analysis, it can be concluded that the use of MRI radiomics for predicting MVI has a high level of accuracy. This non-invasive method can be considered as an alternative approach for evaluating MVI.

Table 1 Advanced magnetic resonance imaging techniques for liver diagnosis: Comparison of clinical applications, advantages, limitations, and developments

Technique(s)	Applications	Advantages	Limitations	Developments
DWI and IVIM	Assessment of liver tumors, diffuse liver lesions, and liver function. Assessment of liver or tumor blood perfusion	Evaluate liver or tumor blood perfusion without the use of contrast agents	Poor reproducibility of IVIM and DWI	2D *b*-M1 acquisition improves reproducibility. The new parameter PDR improves DWI performance
MRE	Diagnosis and staging of liver fibrosis and cirrhosis. Prediction of the recurrence of HCC	Diagnosis of liver fibrosis is not affected by obesity, ascites, inflammation, and etiology	The diagnostic threshold for fibrosis is variable and conflicting	The two-step strategy can screen for liver fibrosis. LS and TS can predict HCC recurrence
CEST	Assessment of tumor metabolism and microenvironment. Monitoring of tumor treatment response	An FDG substitute that does not involve ionizing radiation	Easily affected by other factors. Long scan time	The new reagent 3OMG has unique advantages. Realization of image-guided drug delivery and integration of tumor diagnosis and treatment
CE-MRI	Diagnosis and staging of liver tumors. Detection of liver metastases and diffuse liver lesions	Provides more information about lesions compared to plain MRI. Specific probes enable visualization at the molecular level	Gd chelates can cause allergic reactions and nephrotoxicity	Multi-target probes have the potential to overcome tumor heterogeneity. Potential applications of Mn-based contrast agents in targeted tumor therapy
MRS	Diagnosis and grading of fatty liver and liver fibrosis. Metabolic evaluation of liver and intrahepatic tumors	Provides quantitative data on liver metabolism non-invasively without the use of contrast agents	Low sensitivity of ^{13}C. Accuracy is affected by liver tissue heterogeneity and motion	Cho peak can provide more information. ^{31}P-MRS can differentiate liver cirrhosis etiology and evaluate IRI
HP MR	Providing metabolic, perfusion, and enzymatic information on HCC	DNP improves MR signal by 10000 times. [1-^{13}C] pyruvate has particular value in evaluating tumor metabolism	Current measurement methods still produce inevitable quantitative deviations	HyperPET is expected to elucidate complete glucose metabolism. More hyperpolarized probes are being used. Double-probe HP MR can simultaneously obtain metabolic and perfusion information
MRI radiomics	Diagnosis and prediction of immunohistochemistry features, MVI, liver fibrosis, and hepatitis.	Comprehensive, non-invasive, and quantitative observation of the spatiotemporal heterogeneity of tumors	Poor reproducibility of MRI features. MVI features are variable and conflicting in different studies	Good application value in the differential diagnosis, immunohistochemical feature prediction, and MVI prediction of HCC

CEST: Chemical exchange saturation transfer; CE-MRI: Contrast-enhanced magnetic resonance imaging; Cho: Choline; DNP: Dynamic nuclear polarization; DWI: Diffusion weighted imaging; HCC: Hepatocellular carcinoma; HP: Hyperpolarized; IRI: Ischemia-reperfusion injury; IVIM: Intravoxel incoherent motion; LS: Liver stiffness; MRE: Magnetic resonance elastography; MRI: Magnetic resonance imaging; MRS: Magnetic resonance spectroscopy; MVI: Microvascular invasion; PDR: Perfusion-diffusion ratio; TS: Tumor stiffness; PET: Positron emission tomography; FDG: Fluorodeoxyglucose; 2D: Two-dimensional.

The current limitation of MRI radiomics is the lack of reproducibility in extracting radiomics features. While previous studies have shown good interobserver reproducibility of HCC radiomics features from specific MRI systems, caution is needed when interpreting data in multi-platform radiomics studies as reproducibility can vary greatly between different platforms[101].

Additionally, there is variability and inconsistency in using MRI features to predict MVI in different studies. To combat this, Hong *et al*[102] conducted a meta-analysis of data from 36 studies involving 4410 participants. They identified seven MRI features, namely, large tumor volume, arterial edge enhancement, arterial tumor surrounding enhancement, hypointensity around the tumor in the hepatobiliary phase, irregular margins, multifocality, and low T1 signal, as important predictors of MVI in HCC. These MRI radiomics features are valuable references for future research and of great significance for developing more reliable MVI prediction strategies. Table 1 summarizes various novel MRI technologies' clinical applications, advantages, limitations, and latest developments discussed in this review for the diagnosis of liver diseases. Table 2 lists the diagnostic performance of some MR techniques for the diagnosis of liver diseases.

CONCLUSION

MRI is a promising technology for diagnosing liver diseases due to its non-invasive and radiation-free nature. The development of new technologies such as DWI, IVIM, MRE, CEST, MRS, HP MR, CE-MRI, and radiomics has expanded the capabilities of MRI, allowing for more comprehensive and accurate diagnostic results. Although these technologies have limitations, their role in liver disease diagnosis will continue to improve as they are updated and enhanced. It is important for researchers and clinical doctors to thoroughly study the application value of these new technologies in clinical practice to better guide the diagnosis, treatment, and rehabilitation of liver diseases and ultimately improve patient prognosis.

Table 2 Comparison of performance indicators of new magnetic resonance techniques in diagnosis of liver disease

Technique	Disease	Subjects	Sensitivity (%)	Specificity (%)	NPV (%)	PPV (%)	Ref.
DWI	HCC	34	54.8	90.9	34.5	95.8	[103]
DWI	LF	40	85	82	85	83	[104]
PDR	MT	83	81	77	NA	NA	[18]
MRE	LF	59	69.0	88.2	53.6	93.5	[105]
MRS	Liver steatosis	4715	72.7-88.5	92.0-95.7	NA	NA	[106]
Gd-EOB-DTPA MRI	HCC	77	88.2	96.7	90.6	95.7	[107]
SPIO MRI	HCC	30	66.0	98.0	91.4	90.0	[108]
MRI-PDFF	NAFLD	60	96	100	92.6	89.5	[70]
Radiomics	MVI	50	90	75	NA	NA	[99]
Radiomics	MVI	981	79	81	NA	NA	[100]

DWI: Diffusion weighted imaging; HCC: Hepatocellular carcinoma; LF: Liver fibrosis; MRE: Magnetic resonance elastography; MRI: Magnetic resonance imaging; MRI-PDFF: Magnetic resonance imaging proton density fat fraction; MRS: Magnetic resonance spectroscopy; MT: Malignant tumor; MVI: Microvascular invasion; NA: Not available; NAFLD: Non-alcoholic fatty liver disease; NPV: Negative predictive value; PDR: Perfusion-diffusion ratio; PPV: Positive predictive value; SPIO: Superparamagnetic iron oxide.

FOOTNOTES

Author contributions: Xiao EH was responsible for the review concept and design; Qi YM drafted the manuscript; Xiao EH provided critical revision of the manuscript for important intellectual content; and all authors critically reviewed the content and approved the final version for publication.

Supported by the National Natural Science Foundation of China, No. 81571784; the Provincial Natural Science Foundation of Hunan, No. 2022JJ70142; and the Clinical Research Center for Medical Imaging in Hunan Province, 2020SK4001.

Conflict-of-interest statement: All the authors report no relevant conflicts of interest for this article.

Country/Territory of origin: China

ORCID number: Yi-Ming Qi 0009-0008-4675-3717; En-Hua Xiao 0000-0002-3281-6384.

S-Editor: Wang JJ
L-Editor: Wang TQ
P-Editor: Chen YX

REFERENCES

1 **Moon AM**, Singal AG, Tapper EB. Contemporary Epidemiology of Chronic Liver Disease and Cirrhosis. *Clin Gastroenterol Hepatol* 2020; **18**: 2650-2666 [PMID: 31401364 DOI: 10.1016/j.cgh.2019.07.060]
2 **Dhar D**, Baglieri J, Kisseleva T, Brenner DA. Mechanisms of liver fibrosis and its role in liver cancer. *Exp Biol Med (Maywood)* 2020; **245**: 96-108 [PMID: 31924111 DOI: 10.1177/1535370219898141]
3 **Roehlen N**, Crouchet E, Baumert TF. Liver Fibrosis: Mechanistic Concepts and Therapeutic Perspectives. *Cells* 2020; **9** [PMID: 32260126 DOI: 10.3390/cells9040875]
4 **Harris PS**, Hansen RM, Gray ME, Massoud OI, McGuire BM, Shoreibah MG. Hepatocellular carcinoma surveillance: An evidence-based approach. *World J Gastroenterol* 2019; **25**: 1550-1559 [PMID: 30983815 DOI: 10.3748/wjg.v25.i13.1550]
5 **Donne R**, Lujambio A. The liver cancer immune microenvironment: Therapeutic implications for hepatocellular carcinoma. *Hepatology* 2023; **77**: 1773-1796 [PMID: 35989535 DOI: 10.1002/hep.32740]
6 **Zhou H**, Song T. Conversion therapy and maintenance therapy for primary hepatocellular carcinoma. *Biosci Trends* 2021; **15**: 155-160 [PMID: 34039818 DOI: 10.5582/bst.2021.01091]
7 **Fan Z**, Zhou P, Jin B, Li G, Feng L, Zhuang C, Wang S. Recent therapeutics in hepatocellular carcinoma. *Am J Cancer Res* 2023; **13**: 261-275 [PMID: 36777510]

8 **Tsuge M**, Kawaoka T, Oka S. Factors for the recurrence of hepatocellular carcinoma after hepatic resection. *J Gastroenterol* 2023; **58**: 292-293 [PMID: 36723691 DOI: 10.1007/s00535-023-01962-3]

9 **Ronot M**, Purcell Y, Vilgrain V. Hepatocellular Carcinoma: Current Imaging Modalities for Diagnosis and Prognosis. *Dig Dis Sci* 2019; **64**: 934-950 [PMID: 30825108 DOI: 10.1007/s10620-019-05547-0]

10 **Caroli A**. Diffusion-Weighted Magnetic Resonance Imaging: Clinical Potential and Applications. *J Clin Med* 2022; **11** [PMID: 35743409 DOI: 10.3390/jcm11123339]

11 **Lee S**, Kim SH, Hwang JA, Lee JE, Ha SY. Pre-operative ADC predicts early recurrence of HCC after curative resection. *Eur Radiol* 2019; **29**: 1003-1012 [PMID: 30027408 DOI: 10.1007/s00330-018-5642-5]

12 **Wáng YXJ**. Gender-specific liver aging and magnetic resonance imaging. *Quant Imaging Med Surg* 2021; **11**: 2893-2904 [PMID: 34249621 DOI: 10.21037/qims-21-227]

13 **Li T**, Che-Nordin N, Wáng YXJ, Rong PF, Qiu SW, Zhang SW, Zhang P, Jiang YF, Chevallier O, Zhao F, Xiao XY, Wang W. Intravoxel incoherent motion derived liver perfusion/diffusion readouts can be reliable biomarker for the detection of viral hepatitis B induced liver fibrosis. *Quant Imaging Med Surg* 2019; **9**: 371-385 [PMID: 31032185 DOI: 10.21037/qims.2019.02.11]

14 **Wu B**, Jia F, Li X, Li L, Wang K, Han D. Comparative Study of Amide Proton Transfer Imaging and Intravoxel Incoherent Motion Imaging for Predicting Histologic Grade of Hepatocellular Carcinoma. *Front Oncol* 2020; **10**: 562049 [PMID: 33194630 DOI: 10.3389/fonc.2020.562049]

15 **Tao YY**, Zhou Y, Wang R, Gong XQ, Zheng J, Yang C, Yang L, Zhang XM. Progress of intravoxel incoherent motion diffusion-weighted imaging in liver diseases. *World J Clin Cases* 2020; **8**: 3164-3176 [PMID: 32874971 DOI: 10.12998/wjcc.v8.i15.3164]

16 **Wang J**, Yang Z, Luo M, Xu C, Du M, Liu Y. Value of Intravoxel Incoherent Motion (IVIM) Imaging for Differentiation between Intrahepatic Cholangiocarcinoma and Hepatocellular Carcinoma. *Contrast Media Mol Imaging* 2022; **2022**: 1504463 [PMID: 35615729 DOI: 10.1155/2022/1504463]

17 **Zhu SC**, Liu YH, Wei Y, Li LL, Dou SW, Sun TY, Shi DP. Intravoxel incoherent motion diffusion-weighted magnetic resonance imaging for predicting histological grade of hepatocellular carcinoma: Comparison with conventional diffusion-weighted imaging. *World J Gastroenterol* 2018; **24**: 929-940 [PMID: 29491686 DOI: 10.3748/wjg.v24.i8.929]

18 **Podgórska J**, Pasicz K, Skrzyński W, Gołębiewski B, Kuś P, Jasieniak J, Kiliszczyk A, Rogowska A, Benkert T, Pałucki J, Grabska I, Fabiszewska E, Jagielska B, Kukołowicz P, Cieszanowski A. Perfusion-Diffusion Ratio: A New IVIM Approach in Differentiating Solid Benign and Malignant Primary Lesions of the Liver. *Biomed Res Int* 2022; **2022**: 2957759 [PMID: 35075424 DOI: 10.1155/2022/2957759]

19 **Schmeel FC**. Variability in quantitative diffusion-weighted MR imaging (DWI) across different scanners and imaging sites: is there a potential consensus that can help reducing the limits of expected bias? *Eur Radiol* 2019; **29**: 2243-2245 [PMID: 30488105 DOI: 10.1007/s00330-018-5866-4]

20 **Wáng YXJ**, Wang X, Wu P, Wang Y, Chen W, Chen H, Li J. Topics on quantitative liver magnetic resonance imaging. *Quant Imaging Med Surg* 2019; **9**: 1840-1890 [PMID: 31867237 DOI: 10.21037/qims.2019.09.18]

21 **Simchick G**, Geng R, Zhang Y, Hernando D. b value and first-order motion moment optimized data acquisition for repeatable quantitative intravoxel incoherent motion DWI. *Magn Reson Med* 2022; **87**: 2724-2740 [PMID: 35092092 DOI: 10.1002/mrm.29165]

22 **Li C**, Li R, Zhang W. Progress in non-invasive detection of liver fibrosis. *Cancer Biol Med* 2018; **15**: 124-136 [PMID: 29951337 DOI: 10.20892/j.issn.2095-3941.2018.0018]

23 **Ajmera V**, Loomba R. Imaging biomarkers of NAFLD, NASH, and fibrosis. *Mol Metab* 2021; **50**: 101167 [PMID: 33460786 DOI: 10.1016/j.molmet.2021.101167]

24 **Loomba R**, Adams LA. Advances in non-invasive assessment of hepatic fibrosis. *Gut* 2020; **69**: 1343-1352 [PMID: 32066623 DOI: 10.1136/gutjnl-2018-317593]

25 **Mózes FE**, Lee JA, Selvaraj EA, Jayaswal ANA, Trauner M, Boursier J, Fournier C, Staufer K, Stauber RE, Bugianesi E, Younes R, Gaia S, Lupşor-Platon M, Petta S, Shima T, Okanoue T, Mahadeva S, Chan WK, Eddowes PJ, Hirschfield GM, Newsome PN, Wong VW, de Ledinghen V, Fan J, Shen F, Cobbold JF, Sumida Y, Okajima A, Schattenberg JM, Labenz C, Kim W, Lee MS, Wiegand J, Karlas T, Yılmaz Y, Aithal GP, Palaniyappan N, Cassinotto C, Aggarwal S, Garg H, Ooi GJ, Nakajima A, Yoneda M, Ziol M, Barget N, Geier A, Tuthill T, Brosnan MJ, Anstee QM, Neubauer S, Harrison SA, Bossuyt PM, Pavlides M; LITMUS Investigators. Diagnostic accuracy of non-invasive tests for advanced fibrosis in patients with NAFLD: an individual patient data meta-analysis. *Gut* 2022; **71**: 1006-1019 [PMID: 34001645 DOI: 10.1136/gutjnl-2021-324243]

26 **Patel K**, Sebastiani G. Limitations of non-invasive tests for assessment of liver fibrosis. *JHEP Rep* 2020; **2**: 100067 [PMID: 32118201 DOI: 10.1016/j.jhepr.2020.100067]

27 **Selvaraj EA**, Mózes FE, Jayaswal ANA, Zafarmand MH, Vali Y, Lee JA, Levick CK, Young LAJ, Palaniyappan N, Liu CH, Aithal GP, Romero-Gómez M, Brosnan MJ, Tuthill TA, Anstee QM, Neubauer S, Harrison SA, Bossuyt PM, Pavlides M; LITMUS Investigators. Diagnostic accuracy of elastography and magnetic resonance imaging in patients with NAFLD: A systematic review and meta-analysis. *J Hepatol* 2021; **75**: 770-785 [PMID: 33991635 DOI: 10.1016/j.jhep.2021.04.044]

28 **Agbim U**, Asrani SK. Non-invasive assessment of liver fibrosis and prognosis: an update on serum and elastography markers. *Expert Rev Gastroenterol Hepatol* 2019; **13**: 361-374 [PMID: 30791772 DOI: 10.1080/17474124.2019.1579641]

29 **Gheorghe G**, Bungău S, Ceobanu G, Ilie M, Bacalbaşa N, Bratu OG, Vesa CM, Găman MA, Diaconu CC. The non-invasive assessment of hepatic fibrosis. *J Formos Med Assoc* 2021; **120**: 794-803 [PMID: 32861550 DOI: 10.1016/j.jfma.2020.08.019]

30 **Hsu C**, Caussy C, Imajo K, Chen J, Singh S, Kaulback K, Le MD, Hooker J, Tu X, Bettencourt R, Yin M, Sirlin CB, Ehman RL, Nakajima A, Loomba R. Magnetic Resonance vs Transient Elastography Analysis of Patients With Nonalcoholic Fatty Liver Disease: A Systematic Review and Pooled Analysis of Individual Participants. *Clin Gastroenterol Hepatol* 2019; **17**: 630-637.e8 [PMID: 29908362 DOI: 10.1016/j.cgh.2018.05.059]

31 **Ito H**, Kimura T, Takuro S, Higashitani M, Yamamoto K, Kobayashi D. Liver injury indicators and subsequent cancer development among non-fatty liver population. *Cancer Med* 2023; **12**: 12173-12186 [PMID: 37014815 DOI: 10.1002/cam4.5910]

32 **Tamaki N**, Imajo K, Sharpton SR, Jung J, Sutter N, Kawamura N, Yoneda M, Valasek MA, Behling C, Sirlin CB, Kurosaki M, Izumi N, Nakajima A, Loomba R. Two-Step Strategy, FIB-4 Followed by Magnetic Resonance Elastography, for Detecting Advanced Fibrosis in NAFLD. *Clin Gastroenterol Hepatol* 2023; **21**: 380-387.e3 [PMID: 35123096 DOI: 10.1016/j.cgh.2022.01.023]

33 **Ajmera V**, Kim BK, Yang K, Majzoub AM, Nayfeh T, Tamaki N, Izumi N, Nakajima A, Idilman R, Gumussoy M, Oz DK, Erden A, Quach NE, Tu X, Zhang X, Noureddin M, Allen AM, Loomba R. Liver Stiffness on Magnetic Resonance Elastography and the MEFIB Index and Liver-Related Outcomes in Nonalcoholic Fatty Liver Disease: A Systematic Review and Meta-Analysis of Individual Participants.

Gastroenterology 2022; **163**: 1079-1089.e5 [PMID: 35788349 DOI: 10.1053/j.gastro.2022.06.073]

34 **Yiyi M**, Xiaoqin Q, Lei Z. Spleen Stiffness on Magnetic Resonance Elastography for the Detection of Portal Hypertension: A Systematic Review and Meta-Analysis. *Iran J Public Health* 2022; **51**: 1925-1935 [PMID: 36743372 DOI: 10.18502/ijph.v51i9.10548]

35 **Li M**, Yang H, Liu Y, Zhang L, Chen J, Deng Y, Xiao Y, Zhu J, Yi Z, Hu B, Kuang S, He B, Glaser KJ, Yin M, Venkatesh SK, Ehman RL, Wang J. Comparison of the diagnostic performance of 2D and 3D MR elastography in staging liver fibrosis. *Eur Radiol* 2021; **31**: 9468-9478 [PMID: 34023968 DOI: 10.1007/s00330-021-08053-y]

36 **Catania R**, Lopes Vendrami C, Bolster BD, Niemzcura R, Borhani AA, Miller FH. Intra-patient comparison of 3D and 2D magnetic resonance elastography techniques for assessment of liver stiffness. *Abdom Radiol (NY)* 2022; **47**: 998-1008 [PMID: 34982182 DOI: 10.1007/s00261-021-03355-7]

37 **Higuchi M**, Tamaki N, Kurosaki M, Inada K, Kirino S, Yamashita K, Hayakawa Y, Osawa L, Takaura K, Maeyashiki C, Kaneko S, Yasui Y, Takahashi Y, Tsuchiya K, Nakanishi H, Itakura J, Loomba R, Enomoto N, Izumi N. Longitudinal association of magnetic resonance elastography-associated liver stiffness with complications and mortality. *Aliment Pharmacol Ther* 2022; **55**: 292-301 [PMID: 34927277 DOI: 10.1111/apt.16745]

38 **Zhang L**, Chen J, Jiang H, Rong D, Guo N, Yang H, Zhu J, Hu B, He B, Yin M, Venkatesh SK, Ehman RL, Wang J. MR elastography as a biomarker for prediction of early and late recurrence in HBV-related hepatocellular carcinoma patients before hepatectomy. *Eur J Radiol* 2022; **152**: 110340 [PMID: 35580445 DOI: 10.1016/j.ejrad.2022.110340]

39 **Zhang L**, Li M, Zhu J, Zhang Y, Xiao Y, Dong M, Zhang L, Wang J. The value of quantitative MR elastography-based stiffness for assessing the microvascular invasion grade in hepatocellular carcinoma. *Eur Radiol* 2023; **33**: 4103-4114 [PMID: 36435877 DOI: 10.1007/s00330-022-09290-5]

40 **Singh S**, Venkatesh SK, Wang Z, Miller FH, Motosugi U, Low RN, Hassanein T, Asbach P, Godfrey EM, Yin M, Chen J, Keaveny AP, Bridges M, Bohte A, Murad MH, Lomas DJ, Talwalkar JA, Ehman RL. Diagnostic performance of magnetic resonance elastography in staging liver fibrosis: a systematic review and meta-analysis of individual participant data. *Clin Gastroenterol Hepatol* 2015; **13**: 440-451.e6 [PMID: 25305349 DOI: 10.1016/j.cgh.2014.09.046]

41 **Ward KM**, Aletras AH, Balaban RS. A new class of contrast agents for MRI based on proton chemical exchange dependent saturation transfer (CEST). *J Magn Reson* 2000; **143**: 79-87 [PMID: 10698648 DOI: 10.1006/jmre.1999.1956]

42 **Chan KW**, McMahon MT, Kato Y, Liu G, Bulte JW, Bhujwalla ZM, Artemov D, van Zijl PC. Natural D-glucose as a biodegradable MRI contrast agent for detecting cancer. *Magn Reson Med* 2012; **68**: 1764-1773 [PMID: 23074027 DOI: 10.1002/mrm.24520]

43 **Rivlin M**, Navon G. Molecular imaging of tumors by chemical exchange saturation transfer MRI of glucose analogs. *Quant Imaging Med Surg* 2019; **9**: 1731-1746 [PMID: 31728315 DOI: 10.21037/qims.2019.09.12]

44 **Anemone A**, Capozza M, Arena F, Zullino S, Bardini P, Terreno E, Longo DL, Aime S. In vitro and in vivo comparison of MRI chemical exchange saturation transfer (CEST) properties between native glucose and 3-O-Methyl-D-glucose in a murine tumor model. *NMR Biomed* 2021; **34**: e4602 [PMID: 34423470 DOI: 10.1002/nbm.4602]

45 **Irrera P**, Roberto M, Consolino L, Anemone A, Villano D, Navarro-Tableros V, Carella A, Dastrù W, Aime S, Longo DL. Effect of Esomeprazole Treatment on Extracellular Tumor pH in a Preclinical Model of Prostate Cancer by MRI-CEST Tumor pH Imaging. *Metabolites* 2022; **13** [PMID: 36676972 DOI: 10.3390/metabo13010048]

46 **Schüre JR**, Shrestha M, Breuer S, Deichmann R, Hattingen E, Wagner M, Pilatus U. The pH sensitivity of APT-CEST using phosphorus spectroscopy as a reference method. *NMR Biomed* 2019; **32**: e4125 [PMID: 31322308 DOI: 10.1002/nbm.4125]

47 **Tao Q**, Yi P, Cai Z, Chen Z, Deng Z, Liu R, Feng Y. Ratiometric chemical exchange saturation transfer pH mapping using two iodinated agents with nonequivalent amide protons and a single low saturation power. *Quant Imaging Med Surg* 2022; **12**: 3889-3902 [PMID: 35782235 DOI: 10.21037/qims-21-1229]

48 **Han Z**, Liu G. CEST MRI trackable nanoparticle drug delivery systems. *Biomed Mater* 2021; **16**: 024103 [PMID: 33470986 DOI: 10.1088/1748-605X/abdd70]

49 **Law LH**, Huang J, Xiao P, Liu Y, Chen Z, Lai JHC, Han X, Cheng GWY, Tse KH, Chan KWY. Multiple CEST contrast imaging of nose-to-brain drug delivery using iohexol liposomes at 3T MRI. *J Control Release* 2023; **354**: 208-220 [PMID: 36623695 DOI: 10.1016/j.jconrel.2023.01.011]

50 **Liu G**, Ling J, He L, Xu Y, Chen T, Shi C, Luo L. Theranostic Cancer Treatment Using Lentinan-Coated Selenium Nanoparticles and Label-Free CEST MRI. *Pharmaceutics* 2022; **15** [PMID: 36678748 DOI: 10.3390/pharmaceutics15010120]

51 **Zhou IY**, Catalano OA, Caravan P. Advances in functional and molecular MRI technologies in chronic liver diseases. *J Hepatol* 2020; **73**: 1241-1254 [PMID: 32585160 DOI: 10.1016/j.jhep.2020.06.020]

52 **Zech CJ**, Herrmann KA, Reiser MF, Schoenberg SO. MR imaging in patients with suspected liver metastases: value of liver-specific contrast agent Gd-EOB-DTPA. *Magn Reson Med Sci* 2007; **6**: 43-52 [PMID: 17510541 DOI: 10.2463/mrms.6.43]

53 **Zhou F**, Shang W, Yu X, Tian J. Glypican-3: A promising biomarker for hepatocellular carcinoma diagnosis and treatment. *Med Res Rev* 2018; **38**: 741-767 [PMID: 28621802 DOI: 10.1002/med.21455]

54 **Tahon AM**, El-Ghanam MZ, Zaky S, Emran TM, Bersy AM, El-Raey F, A Z E, El Kharsawy AM, Johar D. Significance of Glypican-3 in Early Detection of Hepatocellular Carcinoma in Cirrhotic Patients. *J Gastrointest Cancer* 2019; **50**: 434-441 [PMID: 29623600 DOI: 10.1007/s12029-018-0095-2]

55 **Liu S**, Wang M, Zheng C, Zhong Q, Shi Y, Han X. Diagnostic value of serum glypican-3 alone and in combination with AFP as an aid in the diagnosis of liver cancer. *Clin Biochem* 2020; **79**: 54-60 [PMID: 32087138 DOI: 10.1016/j.clinbiochem.2020.02.009]

56 **Zhao M**, Liu Z, Dong L, Zhou H, Yang S, Wu W, Lin J. A GPC3-specific aptamer-mediated magnetic resonance probe for hepatocellular carcinoma. *Int J Nanomedicine* 2018; **13**: 4433-4443 [PMID: 30122918 DOI: 10.2147/IJN.S168268]

57 **Luo P**, Wu S, Yu Y, Ming X, Li S, Zuo X, Tu J. Current Status and Perspective Biomarkers in AFP Negative HCC: Towards Screening for and Diagnosing Hepatocellular Carcinoma at an Earlier Stage. *Pathol Oncol Res* 2020; **26**: 599-603 [PMID: 30661224 DOI: 10.1007/s12253-019-00585-5]

58 **Ma XH**, Wang S, Liu SY, Chen K, Wu ZY, Li DF, Mi YT, Hu LB, Chen ZW, Zhao XM. Development and in vitro study of a bi-specific magnetic resonance imaging molecular probe for hepatocellular carcinoma. *World J Gastroenterol* 2019; **25**: 3030-3043 [PMID: 31293339 DOI: 10.3748/wjg.v25.i24.3030]

59 **Davies J**, Siebenhandl-Wolff P, Tranquart F, Jones P, Evans P. Gadolinium: pharmacokinetics and toxicity in humans and laboratory animals following contrast agent administration. *Arch Toxicol* 2022; **96**: 403-429 [PMID: 34997254 DOI: 10.1007/s00204-021-03189-8]

60 **McDonald JS**, McDonald RJ. MR Imaging Safety Considerations of Gadolinium-Based Contrast Agents: Gadolinium Retention and

Nephrogenic Systemic Fibrosis. *Magn Reson Imaging Clin N Am* 2020; **28**: 497-507 [PMID: 33040991 DOI: 10.1016/j.mric.2020.06.001]

61 **Ndiaye D**, Cieslik P, Wadepohl H, Pallier A, Même S, Comba P, Tóth É. Mn(2+) Bispidine Complex Combining Exceptional Stability, Inertness, and MRI Efficiency. *J Am Chem Soc* 2022; **144**: 22212-22220 [PMID: 36445192 DOI: 10.1021/jacs.2c10108]

62 **Cai X**, Zhu Q, Zeng Y, Zeng Q, Chen X, Zhan Y. Manganese Oxide Nanoparticles As MRI Contrast Agents In Tumor Multimodal Imaging And Therapy. *Int J Nanomedicine* 2019; **14**: 8321-8344 [PMID: 31695370 DOI: 10.2147/IJN.S218085]

63 **Lv M**, Chen M, Zhang R, Zhang W, Wang C, Zhang Y, Wei X, Guan Y, Liu J, Feng K, Jing M, Wang X, Liu YC, Mei Q, Han W, Jiang Z. Manganese is critical for antitumor immune responses *via* cGAS-STING and improves the efficacy of clinical immunotherapy. *Cell Res* 2020; **30**: 966-979 [PMID: 32839553 DOI: 10.1038/s41422-020-00395-4]

64 **Zhu X**, Xiong H, Yang P, Wang S, Zhou Q, Zhang P, Zhao Z, Shi S. A pH/GSH dual responsive nanoparticle with relaxivity amplification for magnetic resonance imaging and suppression of tumors and metastases. *Nanoscale* 2023; **15**: 1583-1594 [PMID: 36594591 DOI: 10.1039/d2nr05449c]

65 **Raza S**, Rajak S, Upadhyay A, Tewari A, Anthony Sinha R. Current treatment paradigms and emerging therapies for NAFLD/NASH. *Front Biosci (Landmark Ed)* 2021; **26**: 206-237 [PMID: 33049668 DOI: 10.2741/4892]

66 **Zhang QH**, Zhao Y, Tian SF, Xie LH, Chen LH, Chen AL, Wang N, Song QW, Zhang HN, Xie LZ, Shen ZW, Liu AL. Hepatic fat quantification of magnetic resonance imaging whole-liver segmentation for assessing the severity of nonalcoholic fatty liver disease: comparison with a region of interest sampling method. *Quant Imaging Med Surg* 2021; **11**: 2933-2942 [PMID: 34249624 DOI: 10.21037/qims-20-989]

67 **Caussy C**, Alquiraish MH, Nguyen P, Hernandez C, Cepin S, Fortney LE, Ajmera V, Bettencourt R, Collier S, Hooker J, Sy E, Rizo E, Richards L, Sirlin CB, Loomba R. Optimal threshold of controlled attenuation parameter with MRI-PDFF as the gold standard for the detection of hepatic steatosis. *Hepatology* 2018; **67**: 1348-1359 [PMID: 29108123 DOI: 10.1002/hep.29639]

68 **Kim JW**, Lee CH, Yang Z, Kim BH, Lee YS, Kim KA. The spectrum of magnetic resonance imaging proton density fat fraction (MRI-PDFF), magnetic resonance spectroscopy (MRS), and two different histopathologic methods (artificial intelligence vs. pathologist) in quantifying hepatic steatosis. *Quant Imaging Med Surg* 2022; **12**: 5251-5262 [PMID: 36330193 DOI: 10.21037/qims-22-393]

69 **Yoshizawa E**, Yamada A. MRI-derived proton density fat fraction. *J Med Ultrason (2001)* 2021; **48**: 497-506 [PMID: 34669068 DOI: 10.1007/s10396-021-01135-w]

70 **Yurdaisik I**, Nurili F. Accuracy of Multi-echo Dixon Sequence in Quantification of Hepatic Steatosis. *Cureus* 2020; **12**: e7103 [PMID: 32231898 DOI: 10.7759/cureus.7103]

71 **Ding K**, Liu MR, Huang RS, Lu SJ, Wei X, Wei XX. [A comparative study of 3.0T (1)H-MRS for varying degrees of liver fibrosis in cynomolgus monkeys]. *Zhonghua Gan Zang Bing Za Zhi* 2020; **28**: 766-772 [PMID: 33053977 DOI: 10.3760/cma.j.cn501113-20190212-00044]

72 **Purvis LAB**, Valkovič L, Robson MD, Rodgers CT. Feasibility of absolute quantification for (31) P MRS at 7 T. *Magn Reson Med* 2019; **82**: 49-61 [PMID: 30892732 DOI: 10.1002/mrm.27729]

73 **Liao R**, Tang Z, Li X, Lv L, Yang C, Xiong H, Zhou B, Yu J, Zhang D. Proton Magnetic Resonance Spectroscopy at 3.0T in Rabbit With VX2 Liver Cancer: Diagnostic Efficacy and Correlations With Tumor Size. *Front Oncol* 2022; **12**: 846308 [PMID: 35433458 DOI: 10.3389/fonc.2022.846308]

74 **Seelen LWF**, van den Wildenberg L, van der Kemp WJM, Mohamed Hoesein FAA, Mohammad NH, Molenaar IQ, van Santvoort HC, Prompers JJ, Klomp DWJ. Prospective of (31) P MR Spectroscopy in Hepatopancreatobiliary Cancer: A Systematic Review of the Literature. *J Magn Reson Imaging* 2023; **57**: 1144-1155 [PMID: 35916278 DOI: 10.1002/jmri.28372]

75 **Ko SF**, Chen YL, Sung PH, Chiang JY, Chu YC, Huang CC, Huang CR, Yip HK. Hepatic (31) P-magnetic resonance spectroscopy identified the impact of melatonin-pretreated mitochondria in acute liver ischaemia-reperfusion injury. *J Cell Mol Med* 2020; **24**: 10088-10099 [PMID: 32691975 DOI: 10.1111/jcmm.15617]

76 **Stender S**, Zaha VG, Malloy CR, Sudderth J, DeBerardinis RJ, Park JM. Assessment of Rapid Hepatic Glycogen Synthesis in Humans Using Dynamic (13)C Magnetic Resonance Spectroscopy. *Hepatol Commun* 2020; **4**: 425-433 [PMID: 32140658 DOI: 10.1002/hep4.1458]

77 **Ardenkjaer-Larsen JH**, Fridlund B, Gram A, Hansson G, Hansson L, Lerche MH, Servin R, Thaning M, Golman K. Increase in signal-to-noise ratio of > 10,000 times in liquid-state NMR. *Proc Natl Acad Sci U S A* 2003; **100**: 10158-10163 [PMID: 12930897 DOI: 10.1073/pnas.1733835100]

78 **Ye Y**, Chen M, Chen X, Xiao J, Liao L, Lin F. Clinical Significance and Prognostic Value of Lactate Dehydrogenase Expression in Cervical Cancer. *Genet Test Mol Biomarkers* 2022; **26**: 107-117 [PMID: 35349377 DOI: 10.1089/gtmb.2021.0006]

79 **Granlund KL**, Tee SS, Vargas HA, Lyashchenko SK, Reznik E, Fine S, Laudone V, Eastham JA, Touijer KA, Reuter VE, Gonen M, Sosa RE, Nicholson D, Guo YW, Chen AP, Tropp J, Robb F, Hricak H, Keshari KR. Hyperpolarized MRI of Human Prostate Cancer Reveals Increased Lactate with Tumor Grade Driven by Monocarboxylate Transporter 1. *Cell Metab* 2020; **31**: 105-114.e3 [PMID: 31564440 DOI: 10.1016/j.cmet.2019.08.024]

80 **Bliemsrieder E**, Kaissis G, Grashei M, Topping G, Altomonte J, Hundshammer C, Lohöfer F, Heid I, Keim D, Gebrekidan S, Trajkovic-Arsic M, Winkelkotte AM, Steiger K, Nawroth R, Siveke J, Schwaiger M, Makowski M, Schilling F, Braren R. Hyperpolarized (13)C pyruvate magnetic resonance spectroscopy for in vivo metabolic phenotyping of rat HCC. *Sci Rep* 2021; **11**: 1191 [PMID: 33441943 DOI: 10.1038/s41598-020-80952-4]

81 **Hu S**, Balakrishnan A, Bok RA, Anderton B, Larson PE, Nelson SJ, Kurhanewicz J, Vigneron DB, Goga A. 13C-pyruvate imaging reveals alterations in glycolysis that precede c-Myc-induced tumor formation and regression. *Cell Metab* 2011; **14**: 131-142 [PMID: 21723511 DOI: 10.1016/j.cmet.2011.04.012]

82 **Jensen PR**, Serra SC, Miragoli L, Karlsson M, Cabella C, Poggi L, Venturi L, Tedoldi F, Lerche MH. Hyperpolarized [1,3-13C2]ethyl acetoacetate is a novel diagnostic metabolic marker of liver cancer. *Int J Cancer* 2015; **136**: E117-E126 [PMID: 25156718 DOI: 10.1002/ijc.29162]

83 **Tee SS**, Kim N, Cullen Q, Eskandari R, Mamakhanyan A, Srouji RM, Chirayil R, Jeong S, Shakiba M, Kastenhuber ER, Chen S, Sigel C, Lowe SW, Jarnagin WR, Thompson CB, Schietinger A, Keshari KR. Ketohexokinase-mediated fructose metabolism is lost in hepatocellular carcinoma and can be leveraged for metabolic imaging. *Sci Adv* 2022; **8**: eabm7985 [PMID: 35385296 DOI: 10.1126/sciadv.abm7985]

84 **Eskandari R**, Kim N, Mamakhanyan A, Saoi M, Zhang G, Berisaj M, Granlund KL, Poot AJ, Cross J, Thompson CB, Keshari KR. Hyperpolarized [5-(13)C,4,4-(2)H(2),5-(15)N]-L-glutamine provides a means of annotating in vivo metabolic utilization of glutamine. *Proc Natl Acad Sci U S A* 2022; **119**: e2120595119 [PMID: 35512101 DOI: 10.1073/pnas.2120595119]

85 **Qin H**, Tang S, Riselli AM, Bok RA, Delos Santos R, van Criekinge M, Gordon JW, Aggarwal R, Chen R, Goddard G, Zhang CT, Chen A,

Reed G, Ruscitto DM, Slater J, Sriram R, Larson PEZ, Vigneron DB, Kurhanewicz J. Clinical translation of hyperpolarized (13) C pyruvate and urea MRI for simultaneous metabolic and perfusion imaging. *Magn Reson Med* 2022; **87**: 138-149 [PMID: 34374471 DOI: 10.1002/mrm.28965]

86 **Witney TH**, Lewis DY. Imaging Cancer Metabolism with Positron Emission Tomography (PET). *Methods Mol Biol* 2019; **1928**: 29-44 [PMID: 30725448 DOI: 10.1007/978-1-4939-9027-6_2]

87 **Hansen AE**, Gutte H, Holst P, Johannesen HH, Rahbek S, Clemmensen AE, Larsen MME, Schøier C, Ardenkjaer-Larsen J, Klausen TL, Kristensen AT, Kjaer A. Combined hyperpolarized (13)C-pyruvate MRS and (18)F-FDG PET (hyperPET) estimates of glycolysis in canine cancer patients. *Eur J Radiol* 2018; **103**: 6-12 [PMID: 29803387 DOI: 10.1016/j.ejrad.2018.02.028]

88 **Clemmensen A**, Hansen AE, Holst P, Schøier C, Bisgaard S, Johannesen HH, Ardenkjær-Larsen JH, Kristensen AT, Kjaer A. [(68)Ga]Ga-NODAGA-E[(cRGDyK)](2) PET and hyperpolarized [1-(13)C] pyruvate MRSI (hyperPET) in canine cancer patients: simultaneous imaging of angiogenesis and the Warburg effect. *Eur J Nucl Med Mol Imaging* 2021; **48**: 395-405 [PMID: 32621132 DOI: 10.1007/s00259-020-04881-0]

89 **Hune T**, Mamone S, Schroeder H, Jagtap AP, Sternkopf S, Stevanato G, Korchak S, Fokken C, Müller CA, Schmidt AB, Becker D, Glöggler S. Metabolic Tumor Imaging with Rapidly Signal-Enhanced 1-(13) C-Pyruvate-d(3). *Chemphyschem* 2023; **24**: e202200615 [PMID: 36106366 DOI: 10.1002/cphc.202200615]

90 **Lee PM**, Chen HY, Gordon JW, Zhu Z, Larson PEZ, Dwork N, Van Criekinge M, Carvajal L, Ohliger MA, Wang ZJ, Xu D, Kurhanewicz J, Bok RA, Aggarwal R, Munster PN, Vigneron DB. Specialized computational methods for denoising, B(1) correction, and kinetic modeling in hyperpolarized (13) C MR EPSI studies of liver tumors. *Magn Reson Med* 2021; **86**: 2402-2411 [PMID: 34216051 DOI: 10.1002/mrm.28901]

91 **Lambin P**, Rios-Velazquez E, Leijenaar R, Carvalho S, van Stiphout RG, Granton P, Zegers CM, Gillies R, Boellard R, Dekker A, Aerts HJ. Radiomics: extracting more information from medical images using advanced feature analysis. *Eur J Cancer* 2012; **48**: 441-446 [PMID: 22257792 DOI: 10.1016/j.ejca.2011.11.036]

92 **Wei H**, Shao Z, Fu F, Yu X, Wu Y, Bai Y, Wei W, Meng N, Liu K, Han H, Wang M. Value of multimodal MRI radiomics and machine learning in predicting staging liver fibrosis and grading inflammatory activity. *Br J Radiol* 2023; **96**: 20220512 [PMID: 36341687 DOI: 10.1259/bjr.20220512]

93 **Zheng R**, Shi C, Wang C, Shi N, Qiu T, Chen W, Shi Y, Wang H. Imaging-Based Staging of Hepatic Fibrosis in Patients with Hepatitis B: A Dynamic Radiomics Model Based on Gd-EOB-DTPA-Enhanced MRI. *Biomolecules* 2021; **11** [PMID: 33670596 DOI: 10.3390/biom11020307]

94 **Zhang H**, Guo D, Liu H, He X, Qiao X, Liu X, Liu Y, Zhou J, Zhou Z, Fang Z. MRI-Based Radiomics Models to Discriminate Hepatocellular Carcinoma and Non-Hepatocellular Carcinoma in LR-M According to LI-RADS Version 2018. *Diagnostics (Basel)* 2022; **12** [PMID: 35626199 DOI: 10.3390/diagnostics12051043]

95 **Ameli S**, Venkatesh BA, Shaghaghi M, Ghadimi M, Hazhirkarzar B, Rezvani Habibabadi R, Aliyari Ghasabeh M, Khoshpouri P, Pandey A, Pandey P, Pan L, Grimm R, Kamel IR. Role of MRI-Derived Radiomics Features in Determining Degree of Tumor Differentiation of Hepatocellular Carcinoma. *Diagnostics (Basel)* 2022; **12** [PMID: 36292074 DOI: 10.3390/diagnostics12102386]

96 **Yang F**, Wan Y, Xu L, Wu Y, Shen X, Wang J, Lu D, Shao C, Zheng S, Niu T, Xu X. MRI-Radiomics Prediction for Cytokeratin 19-Positive Hepatocellular Carcinoma: A Multicenter Study. *Front Oncol* 2021; **11**: 672126 [PMID: 34476208 DOI: 10.3389/fonc.2021.672126]

97 **Gu D**, Xie Y, Wei J, Li W, Ye Z, Zhu Z, Tian J, Li X. MRI-Based Radiomics Signature: A Potential Biomarker for Identifying Glypican 3-Positive Hepatocellular Carcinoma. *J Magn Reson Imaging* 2020; **52**: 1679-1687 [PMID: 32491239 DOI: 10.1002/jmri.27199]

98 **Hectors SJ**, Lewis S, Besa C, King MJ, Said D, Putra J, Ward S, Higashi T, Thung S, Yao S, Laface I, Schwartz M, Gnjatic S, Merad M, Hoshida Y, Taouli B. MRI radiomics features predict immuno-oncological characteristics of hepatocellular carcinoma. *Eur Radiol* 2020; **30**: 3759-3769 [PMID: 32086577 DOI: 10.1007/s00330-020-06675-2]

99 **Feng ST**, Jia Y, Liao B, Huang B, Zhou Q, Li X, Wei K, Chen L, Li B, Wang W, Chen S, He X, Wang H, Peng S, Chen ZB, Tang M, Chen Z, Hou Y, Peng Z, Kuang M. Preoperative prediction of microvascular invasion in hepatocellular cancer: a radiomics model using Gd-EOB-DTPA-enhanced MRI. *Eur Radiol* 2019; **29**: 4648-4659 [PMID: 30689032 DOI: 10.1007/s00330-018-5935-8]

100 **Liang G**, Yu W, Liu S, Zhang M, Xie M, Liu M, Liu W. The diagnostic performance of radiomics-based MRI in predicting microvascular invasion in hepatocellular carcinoma: A meta-analysis. *Front Oncol* 2022; **12**: 960944 [PMID: 36798691 DOI: 10.3389/fonc.2022.960944]

101 **Carbonell G**, Kennedy P, Bane O, Kirmani A, El Homsi M, Stocker D, Said D, Mukherjee P, Gevaert O, Lewis S, Hectors S, Taouli B. Precision of MRI radiomics features in the liver and hepatocellular carcinoma. *Eur Radiol* 2022; **32**: 2030-2040 [PMID: 34564745 DOI: 10.1007/s00330-021-08282-1]

102 **Hong SB**, Choi SH, Kim SY, Shim JH, Lee SS, Byun JH, Park SH, Kim KW, Kim S, Lee NK. MRI Features for Predicting Microvascular Invasion of Hepatocellular Carcinoma: A Systematic Review and Meta-Analysis. *Liver Cancer* 2021; **10**: 94-106 [PMID: 33981625 DOI: 10.1159/000513704]

103 **Rimola J**, Forner A, Sapena V, Llarch N, Darnell A, Díaz A, García-Criado A, Bianchi L, Vilana R, Díaz-González Á, Ayuso C, Bruix J, Reig M. Performance of gadoxetic acid MRI and diffusion-weighted imaging for the diagnosis of early recurrence of hepatocellular carcinoma. *Eur Radiol* 2020; **30**: 186-194 [PMID: 31372783 DOI: 10.1007/s00330-019-06351-0]

104 **Razek AA**, Abdalla A, Omran E, Fathy A, Zalata K. Diagnosis and quantification of hepatic fibrosis in children with diffusion weighted MR imaging. *Eur J Radiol* 2011; **78**: 129-134 [PMID: 19926420 DOI: 10.1016/j.ejrad.2009.10.012]

105 **Furlan A**, Tublin ME, Yu L, Chopra KB, Lippello A, Behari J. Comparison of 2D Shear Wave Elastography, Transient Elastography, and MR Elastography for the Diagnosis of Fibrosis in Patients With Nonalcoholic Fatty Liver Disease. *AJR Am J Roentgenol* 2020; **214**: W20-W26 [PMID: 31714842 DOI: 10.2214/AJR.19.21267]

106 **Bohte AE**, van Werven JR, Bipat S, Stoker J. The diagnostic accuracy of US, CT, MRI and 1H-MRS for the evaluation of hepatic steatosis compared with liver biopsy: a meta-analysis. *Eur Radiol* 2011; **21**: 87-97 [PMID: 20680289 DOI: 10.1007/s00330-010-1905-5]

107 **Golfieri R**, Grazioli L, Orlando E, Dormi A, Lucidi V, Corcioni B, Dettori E, Romanini L, Renzulli M. Which is the best MRI marker of malignancy for atypical cirrhotic nodules: hypointensity in hepatobiliary phase alone or combined with other features? Classification after Gd-EOB-DTPA administration. *J Magn Reson Imaging* 2012; **36**: 648-657 [PMID: 22592930 DOI: 10.1002/jmri.23685]

108 **Nishie A**, Tajima T, Ishigami K, Ushijima Y, Okamoto D, Hirakawa M, Nishihara Y, Taketomi A, Hatakenaka M, Irie H, Yoshimitsu K, Honda H. Detection of hepatocellular carcinoma (HCC) using super paramagnetic iron oxide (SPIO)-enhanced MRI: Added value of diffusion-weighted imaging (DWI). *J Magn Reson Imaging* 2010; **31**: 373-382 [PMID: 20099351 DOI: 10.1002/jmri.22059]

Published by **Baishideng Publishing Group Inc**
7041 Koll Center Parkway, Suite 160, Pleasanton, CA 94566, USA
Telephone: +1-925-3991568
E-mail: bpgoffice@wjgnet.com
Help Desk: https://www.f6publishing.com/helpdesk
https://www.wjgnet.com